Single-cycle high-intensity electromagnetic pulse generation in the interaction of a plasma wakefield with regular nonlinear structures

S. S. Bulanov,[1,2] T. Zh. Esirkepov,[3,4] F. F. Kamenets,[3] and F. Pegoraro[5]
[1]*University of Michigan, Ann Arbor, Michigan 48109, USA*
[2]*Institute of Theoretical and Experimental Physics, Moscow, Russia*
[3]*Moscow Institute of Physics and Technology, Dolgoprudnyi, Moscow Region, Russia*
[4]*Kansai Photon Science Institute, JAEA, Kizu, Kyoto, Japan*
[5]*Department of Physics, University of Pisa and CNISM, Pisa, Italy*
(Received 22 November 2005; published 22 March 2006; corrected 28 March 2006)

The interaction of regular nonlinear structures (such as subcycle solitons, electron vortices, and wake Langmuir waves) with a strong wake wave in a collisionless plasma can be exploited in order to produce ultrashort electromagnetic pulses. The electromagnetic field of the nonlinear structure is partially reflected by the electron density modulations of the incident wake wave and a single-cycle high-intensity electromagnetic pulse is formed. Due to the Doppler effect the length of this pulse is much shorter than that of the nonlinear structure. This process is illustrated with two-dimensional particle-in-cell simulations. The considered laser-plasma interaction regimes can be achieved in present day experiments and can be used for plasma diagnostics.

DOI: 10.1103/PhysRevE.73.036408 PACS number(s): 52.38.−r, 42.65.Ky, 52.35.Mw, 52.65.Rr

I. INTRODUCTION

Present day laser technology allows us to generate ultraintense laser pulses with intensities approaching 10^{22} W/cm^2 [1]. The quiver energy of the electrons in the electromagnetic (e.m.) fields of such intense pulses is equal to, or greater than, their rest energy. This regime is achieved for 1 μm wavelength pulses when the pulse intensity exceeds 10^{18} W/cm^2. In this regime the relativistic dynamics of the electrons in the plasma inside which the pulse propagates introduces new types of nonlinear phenomena (see, e.g., the review articles [1] and [2] and the literature quoted therein) that arise from the nonlinearity of the Lorentz force and of the relationship between particle momentum and velocity and, at very large intensities, from nonlinear quantum electrodynamics effects such as electron-positron pair creation [3]. It was soon realized that such nonlinear processes can be harnessed ("relativistic engineering," as introduced in Ref. [4]) in order to concentrate the e.m. radiation in space and in time and produce e.m. pulses of unprecedented high intensity or short duration that can be used to explore ultrahigh-energy-density effects in plasmas. The new possibilities that are made available by nonlinear relativistic optics in plasmas were emphasized by the results presented in [5], where it is shown that synchronized attosecond e.m. pulses and attosecond electron bunches can be produced during the interaction of tightly focused, ultrashort laser pulses with overdense plasmas. The property of nonlinear systems to respond anharmonically to a periodic driving force was exploited in Ref. [6] where the propagation of a high-intensity short laser pulse in a thin wall hollow channel was shown to produce an ultrashort pulse with very short wavelength that propagates outward through the channel walls.

Recently, a different method of generating ultrashort e.m. pulses was proposed in Ref. [7]. This method uses the interaction between a relativistic electromagnetic subcycle soliton and the density modulations of a Langmuir wakefield in a plasma. The mechanism envisaged is based on the results of Ref. [4], where it was shown that when a laser pulse interacts with a breaking wake plasma wave, part of the pulse is reflected in the form of a highly compressed and focused e.m. pulse with an upshifted carrier frequency due to the Doppler effect. The pulse enhancement of the pulse intensity and the pulse compression arise because the electron density modulations in the wake wave act as parabolic relativistic mirrors. In the approach introduced in Ref. [7] the role of laser pulse is taken by a subcycle soliton produced by another laser pulse in the plasma.

Relativistic e.m. subcycle solitons are formed during the interaction of a high-intensity laser pulse with a plasma and a significant fraction of the pulse energy can be trapped in these structures, up to of 30–40 %, as was shown in Ref. [8]. This trapping occurs because, as the laser pulse propagates in the plasma, it loses part of its energy. Since the number of photons in the pulse is approximately conserved, the loss of pulse energy leads to the downshift of the pulse frequency [8,9] below the electron plasma frequency (Langmuir frequency) $\omega_{pe}=(4\pi n_e e^2/m_e)^{1/2}$, where n_e is the electron density, and e and m_e the electron charge and mass. As a result, part of the pulse energy becomes trapped inside electron density cavities in the form of low-frequency radiation. The typical size of these solitons is of the order of the collisionless electron skin depth $d_e=c/\omega_{pe}$. The e.m. fields inside the solitons consist of synchronously oscillating electric and magnetic fields plus a steady electrostatic field which arises from charge separation as electrons are pushed outward by the ponderomotive force of the oscillating fields [10,11]. The development of the analytical theory of intense e.m. solitons in collisionless plasma can be traced in Refs. [8–13]. On a long time scale, the effects of the ion motion become important and the ponderomotive force forms quasineutral cavities in the plasma density, named postsolitons in Ref. [13]. Postsolitons were observed experimentally in Ref. [14] with the use of the proton imaging technique [15].However, for sim-

plicity, in the present paper we shall consider conditions when the effects of the ion motion can be neglected.

On the basis of one-dimensional (1D) analytical calculations, in Ref. [7] it was shown that the e.m. field of the subcycle soliton is partially reflected by the electron density modulations of the wake wave and that the frequency of the reflected pulse is upshifted by a factor $2\gamma_{ph}^2$ as compared to the soliton frequency and its intensity is proportional to γ_{ph}^3, where γ_{ph} is the Lorentz factor corresponding to the phase velocity v_{ph} of the wake wave. It was thus proven that attosecond pulses can in principle be generated by exploiting the soliton-wakefield interaction.

The aim of the present paper is twofold: first, we confirm and qualify the analytical results of Ref. [7] on the basis of two-dimensional (2D) particle-in-cell (PIC) simulations of the interaction of a breaking wake plasma wave with a subcycle soliton; second, we extend the analytical results of Ref. [7] to other types of regular nonlinear structures, an electron vortex and a wakefield, and these two cases are also illustrated with 2D PIC simulations. The parameters of the simulations presented here are deliberately chosen so as to reveal unambiguously the effect of the reflection and the frequency upshift, thus providing a proof-of-principle numerical experiment. Nevertheless, one can see that these effects should occur in present day experiments or can be deliberately realized with contemporary terawatt laser systems.

The paper is organized as follows. The interaction of a wake wave with a soliton is discussed in Sec. II. In the first part of, Sec. II A, we briefly recall the main properties of the reflected pulse, as obtained analytically for a soliton in the 1D approximation. The results of the 2D numerical simulations are presented in Sec. II B, together with the comparison with the 1D analytic results. In the two following Secs. III and IV we present two other possible mechanisms of ultrashort pulse generation which are due to the interaction of a breaking wake plasma wave either an electron vortex or another wake plasma wave oriented in the perpendicular direction. Each of these sections is subdivided into two parts; the first contains the 1D analytical model and the second the results of 2D PIC simulations. Finally, in Sec. V the main results and conclusions are listed.

II. REFLECTION OF THE ELECTROMAGNETIC FIELD OF A SOLITON

A. One-dimensional theory

In this section we recall the 1D results on the form of the e.m. pulse reflected in the soliton-wakefield interaction obtained analytically in Ref. [7].

When an intense short laser pulse interacts with a plasma, it induces a wakefield [16] consisting of nonlinear Langmuir waves with a phase velocity $v_{ph}=\beta_{ph}c$ equal to the group velocity of the laser pulse. If the laser pulse propagates in a low-density plasma, the group velocity is close to the speed of light in vacuum. The nonlinearity of the strong wakefield leads to the steepening of its profile and to the formation of sharply localized maxima (spikes) in the electron density [17]. At wave break (see Ref. [2] and references therein) the electron density in the spikes tends to infinity,

$$n_e(X) = \frac{n_{i0}\beta_{ph}}{\beta_{ph} - \beta_e(X)}, \tag{1}$$

but remains integrable. Here $X=x-v_{ph}t$, n_{i0} is the ion density (equal to the unperturbed electron density n_{e0}), and the ratio β_e between the speed of the electrons and the speed of light varies from $-\beta_{ph}$ to β_{ph}. Close to the wave-breaking conditions, we can write

$$n_e(X) \simeq n_{e0}[1 + \lambda_p \delta(X)]/2, \tag{2}$$

where λ_p is the plasma wavelength in the wave-breaking regime and $\delta(X)$ is the Dirac delta function. This density spike partially reflects a counterpropagating e.m. wave, as shown in Refs. [2,4].

In Ref. [7] the reflection of a 1D, circularly polarized soliton was considered. The soliton was described by the dimensionless vector potential $e\mathbf{A}/(m_e c^2)=A(x,t)(\mathbf{e}_y+i\mathbf{e}_z)$ (see [10]),

$$A(x,t) = \frac{2\varepsilon(\Omega_S)\cosh[\varepsilon(\Omega_S)\omega_{pe}x/c]e^{i\Omega_S t}}{\cosh^2[\varepsilon(\Omega_S)\omega_{pe}x/c] - \varepsilon^2(\Omega_S)}, \tag{3}$$

where $\Omega_S < \omega_{pe}$ is the soliton frequency, and $\varepsilon(\Omega_S)=(1-\Omega_S^2/\omega_{pe}^2)^{1/2}$.

The properties of the reflected pulse were derived by performing a Lorentz transformation to the reference frame where the wake plasma wave is at rest. In this frame the reflection coefficient

$$\rho(\omega') = -\frac{q}{q - i\omega'}, \tag{4}$$

where $q=2\omega_{pe}(2\gamma_{ph})^{1/2}$, derived in Ref. [4] was used for the frequency components obtained by Fourier expanding the soliton amplitude. The form and amplitude of the reflected pulse in the moving frame were then obtained by an inverse Fourier transform followed by the inverse Lorentz transformation of the vector potential. The explicit form of the reflected pulse is presented in Ref. [7] by Eqs. (22)–(28) and by Figs. 2 and 3.

The main conclusion of this analysis is that the amplitudes of the electric and magnetic fields in the reflected pulse are increased by the factor $\gamma_{ph}^{3/2}$, i.e., the pulse intensity is proportional to γ_{ph}^3, while its frequency is upshifted by $2\gamma_{ph}^2$. This scaling indicates that in a tenuous plasma the frequency upshift of the reflected pulse, and its related compression, would be so large that it could lead to the generation of attosecond pulses. The Lorentz factor γ_{ph} of the wakefield generated by a laser pulse in plasma is of the order of $\gamma_{ph} \approx \omega_d/\omega_{pe}$, where ω_d is the frequency of the laser pulse (driver) that generates the wake plasma wave (see Ref. [16]). The frequency upshift is $2\gamma_{ph}^2\Omega_S \approx 2\gamma_{ph}^2\omega_{pe} \approx 2\gamma_{ph}\omega_d$. Thus, for a 1 μm wavelength laser pulse, corresponding to the critical plasma density $n_{cr}=m_e\omega_d^2/4\pi e^2 \approx 10^{21}$ cm^{-3}, the factor $2\gamma_{ph}$that would be required to generate an attosecond reflected pulse is of order 10^3, i.e., the density of the plasma must be order of 4×10^{15} cm^{-3}. Denoting by a_S the dimensionless amplitude of the soliton (defined in terms of the soliton frequency in the laboratory frame), the intensity of the e.m. field in the soliton is given by $I_S \approx (a_S/\gamma_{ph})^2$

$\times 10^{18}$ W/cm^2. Then, the intensity of the reflected e.m. pulse is $I_{ref} \approx \gamma_{ph}^3 I_S = a_S^2 \gamma_{ph} \times 10^{18}$ W/cm^2. According to Ref. [4] the paraboloidal shape of the breaking wake plasma wave focuses the reflected e.m. pulse, further increasing its amplitude. In the case of the soliton, the enhanced scaling of the reflected wave intensity $I_{ref} \approx \gamma_{ph}^5 I_S$, which leads to $\approx a_S^2 \gamma_{ph}^3 \times 10^{18}$ W/cm^2.

B. Two-dimensional PIC simulation

In Ref. [7] the generation of single-cycle electromagnetic pulses during the interaction of the wake Langmuir wave with a relativistic soliton (and in the present paper with other nonlinear structures) is predicted with the help of a one-dimensional model. In order to take into account the effects of multidimensional geometry and strongly nonlinear plasma dynamics, as well as the influence of kinetic effects, we performed 2D PIC simulations using the code REMP based on the PIC method and "density decomposition scheme" [18].

In the simulations presented here, the grid mesh size is $\lambda_d/20$; space and time unit is λ_d and $2\pi/\omega_d$, respectively. Here λ_d and ω_d are the driver laser wavelength and frequency, respectively. In the figures, the electric and magnetic field components are normalized to $m_e \omega_d c/e$ and the electron density is normalized to the critical density $n_{cr} = m_e \omega_d^2 / 4\pi e^2$.

The ions are assumed to form an immobile neutralizing background and thus only the electron motion is taken into account. This approximation is applicable because the typical interaction period is much shorter than the ion response time, e.g., in a hydrogen plasma. In the simulations, the boundary conditions are absorbing for the e.m. field and the quasiparticles. The absorbing condition for the e.m. fields is implemented using the scheme [19] at the cost of an additional (absorbing) edge in the simulation box.

The interaction of a wake wave with a soliton is simulated in a box with size $60\lambda_d \times 40\lambda_d$, including the absorbing edges of thickness $3\lambda_d$. The results are shown in Figs. 1–3. A single relativistic e.m. subcycle soliton is generated by an auxiliary laser pulse with wavelength $\lambda_a = 2\lambda_d$ and dimensionless amplitude $a_a = 0.5$, corresponding to the peak intensity $a_a^2 \times I_1$, where $I_1 = 1.37 \times 10^{18}$ W/cm$^2 \times [1\ \mu\text{m}/\lambda_d^2]$. The pulse is Gaussian with full width at half maximum (FWHM) size (length × waist) $4\lambda_d \times 6\lambda_d$. The auxiliary laser pulse is linearly polarized with its electric field along the z axis; it is generated at the bottom boundary at $t=0$ and propagates along the y axis at $x=20$. The plasma wakefield, which interacts with the soliton, is formed by a Gaussian laser pulse, the driver pulse, with amplitude $a_d = 1.5$ and FWHM size $2\lambda_d \times 12\lambda_d$, starting at time $t=45$ from the left boundary and propagating along the x axis. The driver laser pulse is linearly polarized, its electric field is directed along the y axis. The plasma slab occupies the region $5 \leqslant x \leqslant 35$, $5 \leqslant y \leqslant 35$; it is homogeneous in the direction of the y axis and it has convex parabolic slopes along the x axis from $x=5$ to 11 and from 29 to 35. This plasma-vacuum interface profile is chosen so as to make the laser pulse entrance into the plasma smoother and to avoid a fast wake wave breaking that could happen in the case of a sharp plasma boundary. The electron density at the center of the plasma slab is $n_e = 0.09 n_{cr}$, corresponding to the Langmuir frequency $\omega_{pe} = 0.3$. The number of quasiparticles is 3.24×10^6.

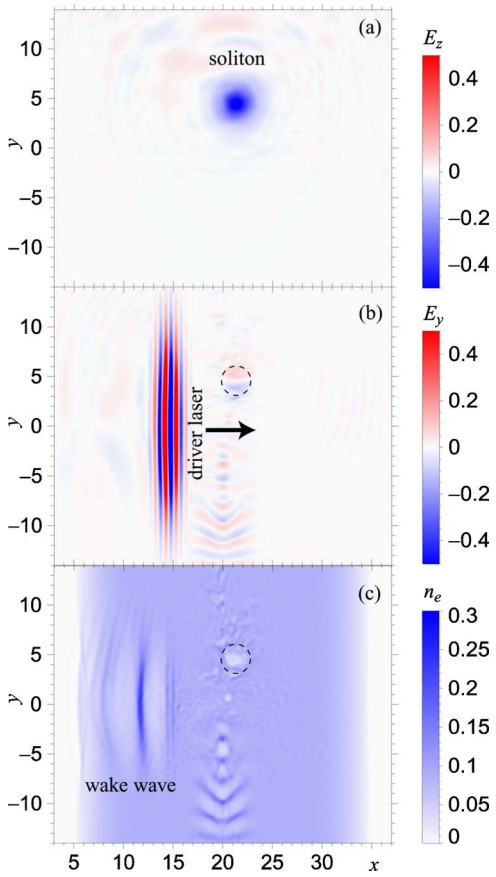

FIG. 1. (Color online) The electric field components E_z (a) and E_y (b) and the electron density n_e (c) before the interaction between the wake wave and the soliton, $t = 61 \times 2\pi/\omega$. The soliton is generated by the auxiliary laser pulse which has already left the simulation box. The dashed circle in (b) and (c) denotes the soliton location.

The phase velocity of the wakefield when it starts to interact with the soliton is $v_{ph} \approx 0.925$, corresponding to the Lorentz factor $\gamma_{ph} \approx 2.63$. The Lorentz factor γ_{ph} is substantially smaller than the ratio between the driver laser frequency and the plasma frequency because, in the case of short pulses, the laser pulse group velocity strongly depends on the pulse size [20]. We note that the characteristic size and time period of the considered regular structures are sufficiently large so that even rather large Lorentz factors lead to relatively low frequencies which can be easily resolved in our simulations.

Figure 1 shows a portion of the simulation box shortly before the interaction. The auxiliary laser pulse has already gone through: in its wake we see a single s-polarized relativistic e.m. subcycle soliton and remnants of a broken wakefield at the bottom of the window. The soliton frequency is well below the unperturbed plasma frequency, $\Omega_S \approx 0.25 \omega_d < \omega_{pe}$. The soliton appears as a region of low electron density, as consistent with the fact that the electrons are pushed outward by the ponderomotive force of the oscillating e.m. fields inside the soliton. Since the driver and the auxiliary

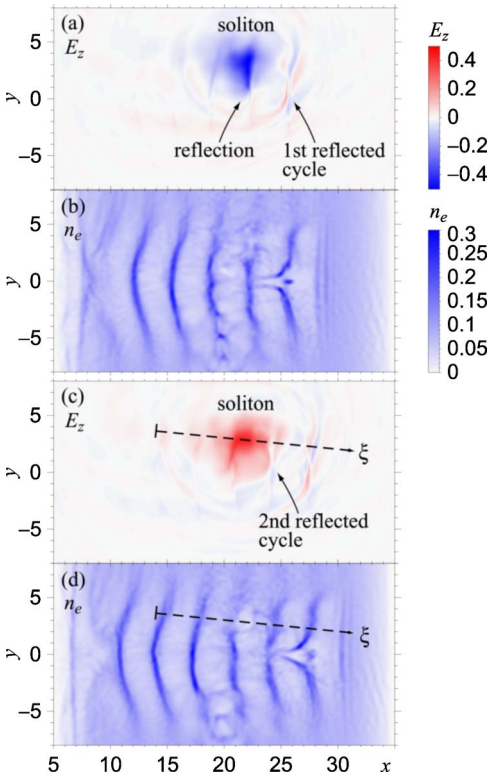

FIG. 2. (Color online) Interaction of the wake wave with the soliton. The electric field component E_z (a), (c) and electron density n_e (b), (d) at $t=76$ (a), (b) and $78\times 2\pi/\omega$ (c), (d). Dashed line ξ: see next figure.

laser pulses have different polarizations and the soliton inherits its polarization from the auxiliary laser, it is easy to distinguish the e.m. field reflected from the soliton in the distribution of the E_z component. The driver laser pulse induces a strong wakefield which is seen in the electron density distribution as a series of wide regions of rarefaction alternating with thin horseshoe-shaped regions of compression. This is the typical pattern of the wake of a Gaussian intense short laser pulse. Regions of compression correspond to spikes (cusps) in the longitudinal profile of the electron

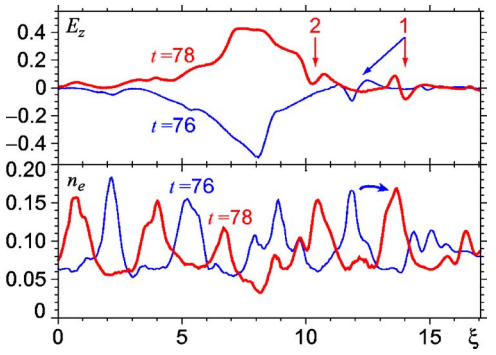

FIG. 3. (Color online) Reflection of the soliton electromagnetic field by the electron density cusps. The electric field component E_z and electron density n_e at $t=76,78\times 2\pi/\omega$ along the dashed line ξ on the previous figure. The first and second reflected pulses are marked with "1" and "2," respectively.

density, which is well explained by the one-dimensional theory [17]. These density cusps play the role of semitransparent mirrors, moving with relativistic velocity.

Figures 2 and 3 show the interaction of the density cusps in the wake of the driver pulse with the soliton. In Fig. 2 the z component of electric field and the electron density are shown. The wake wave of the driver is close to the wave-breaking regime. Each electron density maximum (each cusp) in the wake acts as a fast moving semitransparent parabolic mirror that partially reflects the e.m. fields of the soliton as it propagates through the soliton. The process is repeated when the subsequent cusps of the electron density propagate through the soliton. Thus a set of short e.m. pulses is formed. We note that individual electrons perform an oscillatory motion, while the electron density cusps exhibit a progressive motion. According to Maxwell equations this electric charge density, and the associated electric current density, determine the e.m. field evolution and reflection. Even though the electron density cusp is substantially distorted as it moves through the soliton, it recovers after leaving the soliton. Surprisingly, this transient distortion of the cusp when crossing the soliton does not prevent the formation of well pronounced single-cycle pulses, and one can see the process of their generation even inside the soliton. We also note that the single-cycle pulses move faster than the electron ridge.

The frequency of the fields in the reflected single-cycle e.m. pulses is upshifted and their longitudinal size is much smaller than the size of the soliton, as it can be clearly seen from Fig. 3. These simulation results confirm the physical mechanism investigated analytically in Ref. [7], as summarized in Sec. II A. Since the soliton is not exactly positioned at the crossing of laser pulse axes, the reflected pulse is not exactly directed along the x axis. This is a consequence of the parabolic profile of the wakefield: as the pulse is reflected by the upper wing of parabola it propagates at an angle with respect to the x axis.

Let us now estimate the parameters of the reflected single-cycle pulse according to the results of the 1D analytic calculations, using the initial conditions of the numerical simulations. In this case $\gamma_{ph}\approx 2.63$. The intensity of the soliton is $I_S=(a_S\Omega_S/\omega_d)^2 I_1\approx 0.016 I_1$, where $a_S\approx 0.5$ is the soliton amplitude. The reflected pulse intensity according to the 1D analytic prediction is $I_{ref}^{1D}=\gamma_{ph}^3 I_S\approx 0.28 I_1$. The reflected pulse amplitude, as seen from the results of numerical simulations, is $a_{ref}\approx 0.14$. Then $I_{ref}=(2\gamma_{ph}^2 a_{ref}\Omega_S/\omega_d)^2 I_1\approx 0.23 I_1$, which is in reasonable agreement with the 1D theoretical analysis and reproduce well the predicted scaling.

III. REFLECTION OF THE ELECTROMAGNETIC FIELD OF THE ELECTRON VORTEX

A. One-dimensional theory

Ultrashort electromagnetic pulses can also be generated in the interaction of a breaking wake plasma wave with different types of regular structures besides solitons, such as electron vortices, wake fields, etc. In this section we consider the interaction of a wakefield with an electron vortex. For the sake of illustration, in the following we will employ a sim-

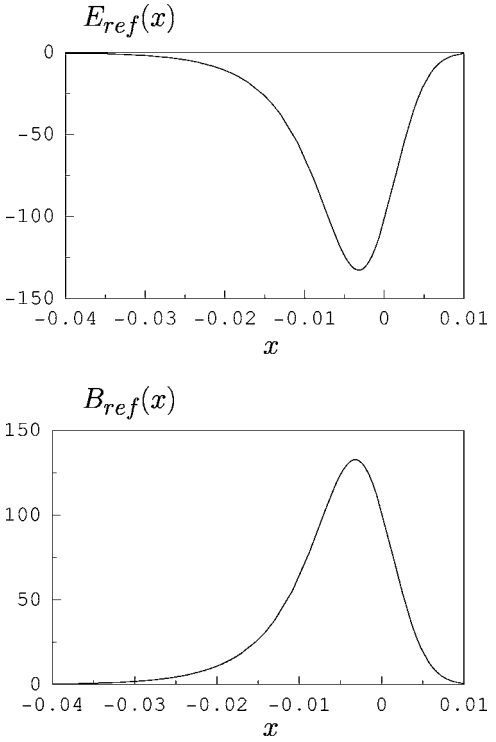

FIG. 4. The electric E_{ref} and magnetic B_{ref} fields of the reflected pulse in the vortex-wakefield interaction as obtained from the one-dimensional theory vs the spatial coordinate x at $t=0$, for $\gamma_{ph}=10$. The fields are measured in units of the initial vortex field and x is measured in units of c/ω_{pe}.

plified representation of their spatial structure.

An electron vortex is characterized by a quasistatic magnetic field generated by the current of electrons circulating in a plasma with steady ions. Contrary to hydrodynamic vortices in ideal fluids, electron vortices in a plasma have a characteristic spatial scale that is given approximately by the plasma collisionless skin depth $d_e=c/\omega_{pe}$. The generation of electron vortices, together with their associated magnetic field, by ultraintense laser pulses in plasmas is observed routinely in computer simulations [21] (see also [2,22] and [23]).

For the sake of simplicity we consider a 1D configuration, which corresponds to magnetic "ribbons" as discussed, e.g., in [21,22], take the magnetic field to be perpendicular to the direction of the wake wave, and assume its profile to be Gaussian, i.e.,

$$B = B_0 \exp(-x^2/d_e^2). \tag{5}$$

Following the procedure proposed in Ref. [7], we perform the Lorentz transformation to the reference frame where the wakefield is at rest and the magnetic field of the electron vortex appears as an incident e.m. pulse. Then, we Fourier transform the incident pulse and use the reflection and transition coefficients derived in Ref. [4]. By inverting the Fourier transform and by performing the Lorentz transformation back to the laboratory frame, we obtain that the shape of the reflected pulse is given by (see Fig. 4)

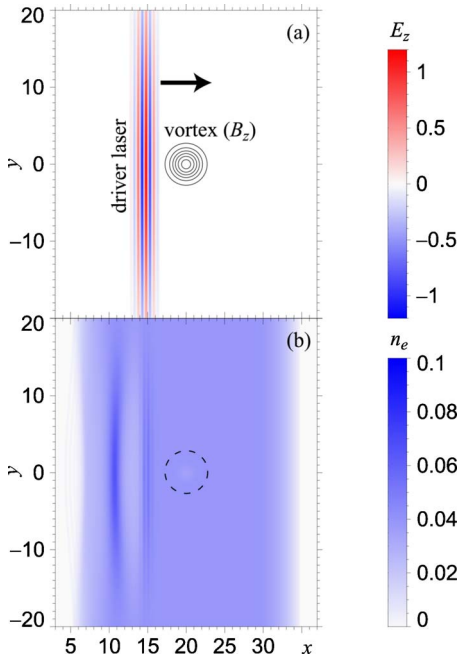

FIG. 5. (Color online) The electric field component E_z (color scale) and contours of the magnetic field component B_z for values $B_z=(1,2,3,4,5,6)\times10^{-2}$ (a) and the electron density n_e (b) at $t=27\times2\pi/\omega$. The dashed circle denotes the electron vortex location.

$$\frac{E_{ref}}{\gamma_{ph}^{3/2}B_0} = (8\pi)^{1/2}\exp(\varphi^2-\psi)\left[1-\mathrm{erf}\left(\varphi-\frac{\psi}{2\varphi}\right)\right], \tag{6}$$

where

$$\varphi = 2^{1/2}/\beta_{ph}\gamma_{ph}^{1/2},$$

$\psi=4\sqrt{2}\gamma_{ph}^{3/2}\omega_{pe}(t-x/c)$and $\mathrm{erf}(x)=\frac{2}{\sqrt{\pi}}\int_0^x\exp(-t^2)dt$ is the error function. As expected, the field of the reflected pulse scales for large γ_{ph} as $\gamma_{ph}^{3/2}$, and thus its intensity scales as γ_{ph}^3. However the reflected pulse width has a more complicated scaling. As can be clearly seen from Fig. 4, where the electric and magnetic fields of the reflected pulse are shown, we have two different scales $1/\gamma_{ph}^2$ and $1/\gamma_{ph}^{3/2}$, and the front of the reflected pulse is much steeper than its tail. This behavior can also be deduced from Eq. (6) since the width of the front of the pulse is determined by the expression in square brackets where the argument of the error function scales as $1/\gamma_{ph}^2$. On the contrary, the form of the tail is determined by the factor $\exp(-\psi)$where ψ is proportional to $\gamma_{ph}^{3/2}$.

B. Two-dimensional PIC simulation

The interaction of a wake wave with an electron vortex, associated with a quasi-stationary transverse magnetic field, is simulated in a box with size $50\lambda_d\times80\lambda_d$, including absorbing edges of thickness $2\lambda_d$. The results are shown in Figs. 5–7. The electron vortex is prepared by introducing a magnetic field B_z which increases gradually from $t=0$ to 10. After $t=10$, a self-consistent quasistationary electron fluid vortex is formed with its corresponding magnetic field dis-

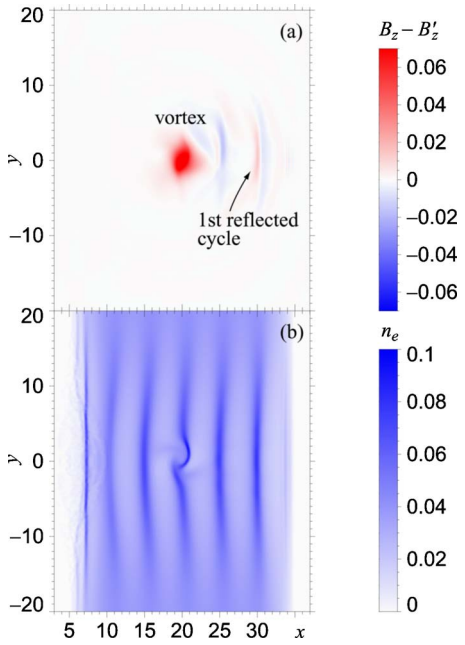

FIG. 6. (Color online) Interaction of the wake wave with the electron vortex, $t=47\times 2\pi/\omega$. (a) The difference between the magnetic field component B_z and B'_z, where B'_z is obtained from the simulation without the vortex. (b) The electron density.

tribution $B_z=0.066\exp[-(x-20)^2/4-y^2/4]$; Fig. 5. The shape of the plasma slab is the same as in the previous simulation (Sec. II B) except that its transverse size (along the y axis) is $70\lambda_d$ and the maximum electron density is $n_e=0.04n_{cr}$. The number of quasiparticles is 3.4×10^6. A Gaussian, linearly polarized (E in the z direction), driver laser pulse with amplitude $a_d=1.2$ and FWHM size $2\lambda_d\times 30\lambda_d$, starts from $t=10$ from the left boundary, propagates along the x axis, and induces a plasma wakefield which interacts with the electron vortex. The phase velocity of the wakefield is $v_{ph}\approx 0.965$, so that the Lorentz factor is $\gamma_{ph}\approx 3.81$. A large waist of the driver laser pulse is chosen to make the interpretation of the reflection easier.

Figure 6 shows the z component of magnetic field and the electron density during the interaction. The wake wave itself

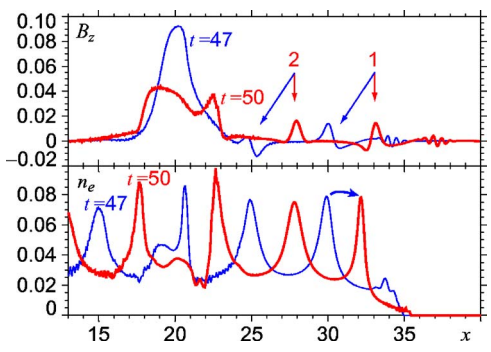

FIG. 7. (Color online) Reflection of the electromagnetic field of the electron vortex by electron density cusps. The magnetic field component B_z and electron density n_e at $t=47,50\times 2\pi/\omega$ along the x axis at $y=0$. The first and second reflected pulses are marked with "1" and "2," respectively.

has a transverse magnetic field B'_z which arises due to the wake wave curvature. The wake wave bending implies that, in addition to the longitudinal oscillatory motion, electrons move toward the wake wave axis, thus inducing a weak transverse magnetic field which is maximum on the periphery, in the regions of the electron density compression. Eventually, this effect results in a so-called transverse wave break of the wakefield [24]. Although the magnetic field of the wake wave does not prevent us from distinguishing the e.m. pulses reflected from the vortex easily, nevertheless, in order to improve the presentation, in Fig. 6 we show the quantity $B_z-B'_z$, where B_z and B'_z are the magnetic field components seen, respectively, in two simulations—one as described in this section, and the other performed with the same parameters but without the vortex (i.e., with no initial magnetic field). Thus a "pure" reflection of the e.m. field of the vortex, resulting in formation of single-cycle pulses, can be seen. In Fig. 7 the magnetic field component B_z and electron charge density n_e are shown along the x axis at $y=0$, where the magnetic field of the wake wave is exactly zero.

As in the case of the interaction of the wake wave and a soliton, the electron density cusp is substantially distorted as it moves through the vortex and it recovers after passing the vortex (Figs. 6 and 7). As in the soliton case this transient distortion of the cusp does not affect the shape of the resulting single-cycle pulses. We also note that the electron vortex is distorted due to modulations of the electron density in the wake wave. The size of the vortex and the magnitude of corresponding magnetic field change so that the angular momentum and vorticity of the electron fluid are preserved.

IV. REFLECTION OF THE ELECTROMAGNETIC FIELD OF THE PLASMA WAKE WAVE

A. One-dimensional theory

Let us now consider the interaction of two wake plasma waves which are oriented perpendicularly with respect to each other. We assume that the amplitude of one of the two waves (the first) is much smaller than that of the other (the second) and thus neglect the action of the first on the second wave. In this scheme the first wake wave provides the electric field which is (partially) reflected by the relativistic mirrors represented by the electron density spikes of the second wake wave.

We assume that the electric field of the first wake wave is directed along the y axis and its spatial dependence along the x axis, i.e., along the propagation direction of the electron density spikes of the second wave (the mirrors), can be modeled as a two-step function with a constant amplitude plateau in between. We can choose the parameters of the e.m. pulse that generates the first wake wave in such a way that the wavelength of the latter at breaking is much larger than its transverse size (the size of the amplitude plateau) which is assumed to be given by the characteristic scale of nonlinear plasma structures $d_e=c/\omega_{pe}$, i.e., such that $2\sqrt{2\gamma_{ph}}c/\pi\omega_{pe}\geqslant d_e=c/\omega_{pe}$. In this case the electric field of the first wave during its reflection from the second wake wave can be taken to be essentially a function of x only and to be of the form

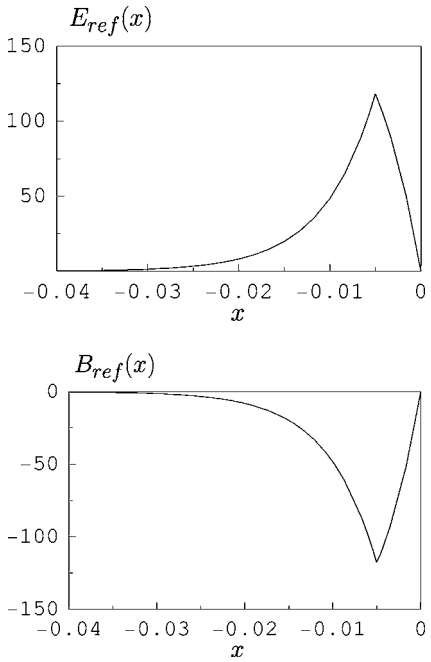

FIG. 8. The electric E_{ref} and magnetic B_{ref} fields of the reflected pulse in the wakefield-wakefield interaction vs the spatial coordinate x at $t=0$ for $\gamma_{ph}=10$. The fields are measured in units of the initial field strength of the first wakefield; x is measured in units of c/ω_{pe}.

$$E_w = E_0\theta(x)\,\theta(c/\omega_{pe}-x). \tag{7}$$

Following the same procedure as in the previous section, we obtain for the electric field of the reflected pulse

$$E_{ref} = 2\gamma_{ph}^2 E_0\theta(t-x/c)\left[1-\exp(-\psi)\right. \\ \left. -\left[1-\exp\left(\frac{2\sqrt{2}}{\sqrt{\gamma_{ph}}}-\psi\right)\right]\theta\left((t-x/c)-\frac{1}{2\omega_{pe}\gamma_{ph}^2}\right)\right] \tag{8}$$

(see Fig. 8). Here we also see the interplay of two scales $1/\gamma_{ph}^2$ and $1/\gamma_{ph}^{3/2}$ as in Fig. 4. The first one is connected with the width of the reflected pulse front and follows from the distance between the arguments of the two theta functions. The second one determines the tail width and arises from the $\exp(-\psi)$ term in Eq. (8). The reflected pulse field strength reaches its maximum value

$$E_{max} = 2\gamma_{ph}^2\left[1-\exp\left(\frac{2\sqrt{2}}{\sqrt{\gamma_{ph}}}\right)\right]E_0 \tag{9}$$

at $t-x/c=1/(2\gamma_{ph}^2\omega_{pe})$. For large values of γ_{ph} we obtain

$$E_{max} = 4\sqrt{2}\gamma_{ph}^{3/2}E_0. \tag{10}$$

Thus the amplitude of the e.m. field scales as $\gamma_{ph}^{3/2}$, similarly to the case of the reflection of the soliton and of the electron vortex from a breaking wake plasma wave. This scaling can be explained as follows. First, the e.m. field after reflection by the moving mirror acquires a factor proportional to γ_{ph}^2 due to Doppler effect. This can be easily shown with the two Lorentz transformations—to the proper reference frame of the mirror and back—to the laboratory reference frame (the vector potential representing the e.m. field is perpendicular to the direction of propagation of the mirror and thus remains unchanged while the frequencies and wave numbers are upshifted by a factor γ_{ph}^2). Second, the reflection coefficient of the electron density spike is proportional to $\gamma_{ph}^{-1/2}$. These two facts result in the overall $\gamma_{ph}^{3/2}$ factor. Actually, as discussed in the description of Figs. 4 and 8, the spatial scaling of the reflected pulse is not simply accounted for by the frequency and wave number upshift. In these two figures we observe two scales $1/\gamma_{ph}^2$ and $1/\gamma_{ph}^{3/2}$. The first scale is a consequence of the Doppler effect and is connected with the frequency and wave number upshift. It manifests itself in the frequency of the reflected pulse from a soliton and in the scale of the front parts of the reflected pulses from a vortex and a wakefield. The second scale manifests itself, in the case of the soliton, in the size of the reflected pulse envelope and, in the case of the vortex and of the wakefield, in the decay length of the reflected pulse tail. This second scale is due to the preferential reflection of the low-frequency part of the field, i.e., to the fact that the reflectivity of the mirror increases and tends to unity for e.m. radiation with frequency of the order of $\gamma_{ph}^{1/2}\omega_{pe}$ in theproper frame of the mirror (or $\gamma_{ph}^{3/2}\omega_{pe}$, in the laboratory frame).

Finally, we should also note that ultrashort e.m. pulses can be generated when a wake wave interacts with plasma in a self-focusing channel [25] (see also, e.g., [26] and references therein). In a self-focusing channel, an electric field is present due to charge separation and can be transformed into an ultrashort e.m. pulse, similarly to the soliton, vortex, or wake wave.

B. Two-dimensional PIC simulation

In order to show the interaction of a wake wave with another (weak) wake wave, we performed a simulation with the same simulation box and plasma distribution as in the previous cases (Sec. III B) except for the maximum electron density which is now $n_e=0.01n_{cr}$. The results are shown in Figs. 9–11. Two laser pulses, which are linearly polarized (E along the z-axis) and propagate in perpendicular directions, induce two plasma wakes, Fig. 9. The first, auxiliary, laser pulse with Gaussian shape, amplitude $a_a=0.7$, wavelength $\lambda_a=\lambda_d$, and FWHM size (length$\times$waist) $2.5\lambda_d\times 10\lambda_d$, starts at $t=0$ from the bottom boundary, propagates in the direction of the y axis at $x=20$ and induces a weak wakefield with a longitudinal electric field directed along the y axis. In Fig. 9 this weak wake wave is seen as a vertical periodic structure. The second laser pulse (driver) is switched on at $t=70$ on the left boundary. Its amplitude is $a_d=2$ and size is $2\lambda_d\times 50\lambda_d$. The driver pulse has a Gaussian profile in the direction of the x axis; along the y axis its shape is a smooth centrosymmetric, piecewise polynomial with sizes of adjacent parts 8,34,8. The central part is constant; the profile of the first slope is defined by $(3-2\eta)\eta^2$, $\eta=y/8$. We chose such the shape of the driver laser pulse so as to ensure the transverse homogeneity of the induced wakefield in the region -17

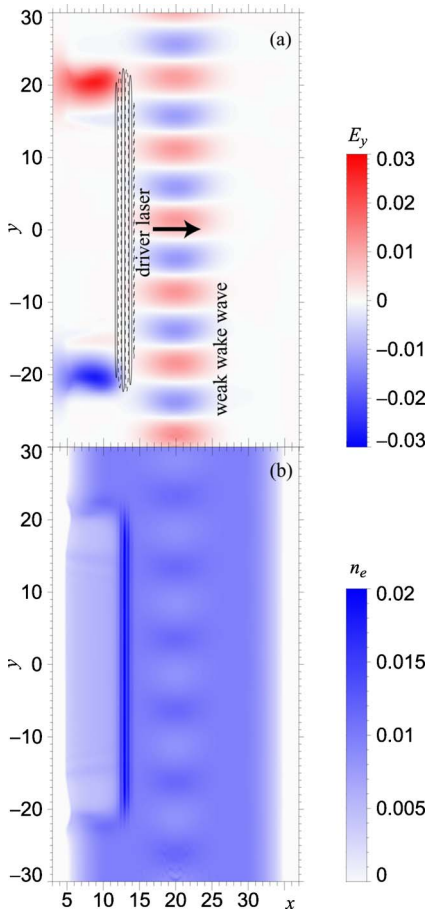

FIG. 9. (Color online) (a) The electric field component E_y (color-scale) and contours of the component E_z for values $E_z=-0.5$ (dashed) and $+0.5m_e\omega c/e$ (solid) and (b) the electron density n_e at $t=85\times 2\pi/\omega$. Here and in the following figures all quantities are given in dimensionless units. The weak wake wave, seen as a vertical periodic structure, is generated by the auxiliary laser pulse which has already left the simulation box. In the wake from the driver laser pulse, the E_y is zero in the region $-10<y<10$, which corresponds to the homogeneous part of the driver.

$<y<17$, and thus to obtain a plasma wake with zero transverse electric field in this region. In other words, the quasi-one-dimensional part of the driver induces the wakefield which is also quasi-one-dimensional. With such a configuration, in the distribution of the E_y component inside the region $-17<y<17$, we see, in principle, only the electric field of the weak wakefield, induced by the auxiliary laser pulse. The wakefield from the driver has phase velocity $v_{ph}\approx 0.982$ and the Lorentz factor $\gamma_{ph}\approx 5.32$.

Figure 10 shows the y component of electric field and electron density at three moments of time with period approximately equal to the period of the plasma wake wave induced by the driver laser pulse. The driver is represented by contours of the z component of electric field. In Fig. 11 the electric field component E_y and electron charge density n_e are shown along the x axis at $y=0$.

Again we note that, as in the case of the interaction of the wake wave with a soliton and vortex, the electron density cusp is distorted inside the weak wake wave, but is almost

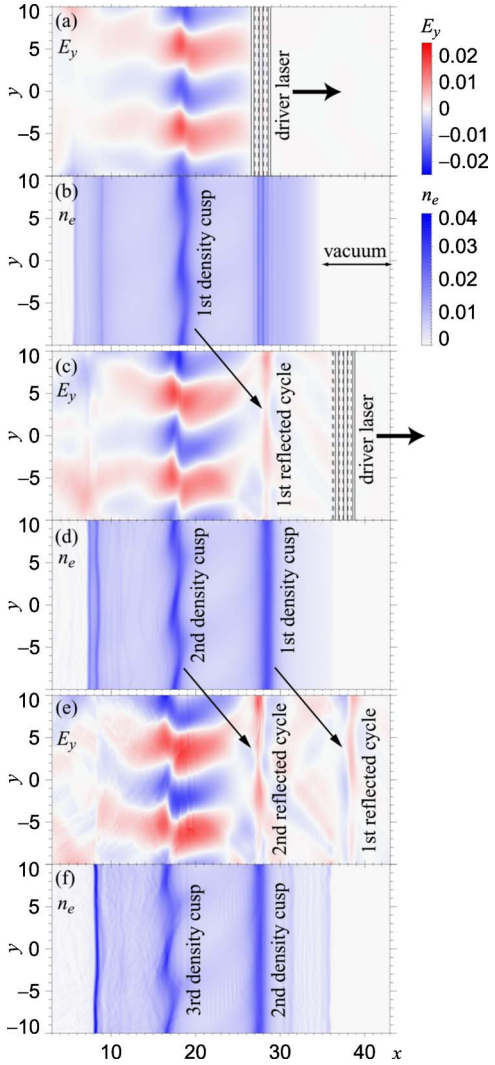

FIG. 10. (Color online) Interaction of the wake wave with the weak wave, shown in the portion of the simulation box $-10<y<10$ corresponding to the quasi-one-dimensional part of the wakefield from the driver. The electric field component E_y (a), (c), (e) and electron density n_e (b), (d), (f) at $t=100$ (a), (b), 110 (c), (d), and $120\times 2\pi/\omega$ (e), (f). The driver laser pulse is represented by contours of the electric field component E_z in the same way as in the previous figure.

restored when it moves outside (Figs. 10 and 11). Even though the electron density cusp seems curved when it is under the influence of the weak wake wave, the single-cycle pulse reflected by this cusp appears to be flat.

As in the cases of other nonlinear structures described above, each density cusp reflects single-cycle e.m. pulse whose frequency is upshifted and whose intensity is increased due to the Doppler effect. A complication that is not included in the presented 1D theory arises from the fact that the weak wake wave, which is (partially) reflected by the "mirrors" of the wake from the driver, has almost the same phase velocity as these mirrors.

V. CONCLUSION

Our analytical model and two-dimensional particle-in-cell simulations show that during the interaction of regular non-

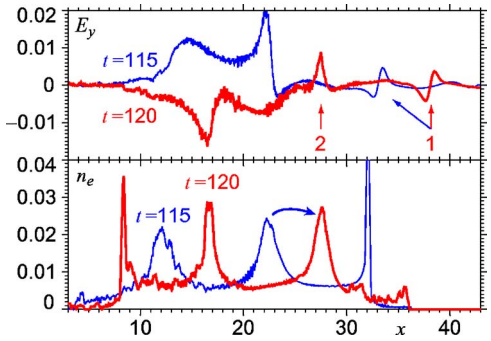

FIG. 11. (Color online) Reflection of the electromagnetic field of the weak wake wave by electron density cusps of the wake wave from the driver. The electric field component E_y and electron density n_e at $t=(115,120)\times 2\pi/\omega$ along the x axis at $y=0$. The first and second reflected pulses are marked with "1" and "2," respectively.

linear structures (such as subcycle solitons, electron vortices, and wake Langmuir waves) with a strong wake wave in a collisionless plasma a train of single-cycle intense electromagnetic pulses is generated. This effect can be exploited in order to produce ultrashort intense e.m. pulses with presently available lasers. The results presented here confirm and extend the analytical results obtained in Ref. [7].

The modulations of electron density in the strong wake wave, which is close to the wave-breaking regime, have the shape of spikes. Each spike acts as a semitransparent mirror moving with a relativistic velocity, corresponding to the phase velocity of the wake wave. Such a mirror partially reflects the electromagnetic field of a nonlinear structure and thus generates an electromagnetic pulse. As predicted in Ref. [7], the reflected pulse consists of a single-cycle oscillation and, as compared to the e.m. field of the nonlinear structure, the reflected pulse has an upshifted frequency and an increased intensity. The reflected pulse intensity occurs as a result of frequency upshift, due to Doppler effect, and because of the parabolic profile of the wake wave.

Using an analytical approach, we have shown that in the three cases considered here of nonlinear structures—a subcycle soliton, an electron vortex, and a wake wave—the amplitude of the e.m. pulse, reflected by a relativistic flying mirror, scales as $\gamma_{ph}^{3/2}$, due to a similarity of the reflection process in all three cases. The reflection leads to a frequency and wave number upshift which scales as γ_{ph}^2 and to the formation of an additional spatial scale proportional to $1/\gamma_{ph}^{3/2}$.

Since in all the above cases of wakefield interaction with nonlinear regular structures in a plasma, single-cycle e.m. pulses are emitted with a characteristic frequency, duration, and polarization, their emission represents an important process to be used for diagnostics of laser-plasma interactions.

ACKNOWLEDGMENTS

The authors would like to acknowledge fruitful discussions with A. Maksimchuk and V. Yanovsky. This work is partially supported by INTAS Grant No. 001-0233 and the Federal Program of the Russian Ministry of Industry, Science and Technology Grant No. 40.052.1.1.1112. It was also partially supported by RFBR Grant No. SS-2328.2003.2.

[1] G. A. Mourou, C. P. J. Barty, and M. D. Perry, Phys. Today **51**(1), 22 (1998).
[2] S. V. Bulanov *et al.*, in *Reviews of Plasma Physics*, edited by V. D. Shafranov (Kluwer Academic/Plenum Publishers, New York, 2001), Vol. 22, p. 227.
[3] S. S. Bulanov, Phys. Rev. E **69**, 036408 (2004); S. S. Bulanov, A. M. Fedotov, and F. Pegoraro, *ibid.* **71**, 016404 (2005).
[4] S. V. Bulanov, T. Esirkepov, and T. Tajima, Phys. Rev. Lett. **91**, 085001 (2003).
[5] N. M. Naumova, J. A. Nees, I. V. Sokolov, B. Hou, and G. A. Mourou, Phys. Rev. Lett. **92**, 063902 (2004); N. Naumova, I. Sokolov, J. Nees, A. Maksimchuk, V. Yanovsky, and G. Mourou, *ibid.* **93**, 195003 (2004); N. M. Naumova, J. A. Nees, and G. A. Mourou, Phys. Plasmas **12**, 056707 (2005).
[6] S. V. Bulanov, T. Zh. Esirkepov, N. M. Naumova, and I. V. Sokolov, Phys. Rev. E **67**, 016405 (2003).
[7] A. V. Isanin, S. S. Bulanov, F. F. Kamenets, and F. Pegoraro, Phys. Lett. A **337**, 107 (2005).
[8] S. V. Bulanov, I. N. Inovenkov, V. I. Kirsanov, N. M. Naumova, and A. S. Sakharov, Phys. Fluids B **4**, 1935 (1992); S. V. Bulanov, T. Zh. Esirkepov, F. F. Kamenets, and N. M. Naumova, Plasma Phys. Rep. **21**, 550 (1995); S. V. Bulanov, T. Zh. Esirkepov, N. M. Naumova, F. Pegoraro, and V. A. Vshivkov, Phys. Rev. Lett. **82**, 3440 (1999); T. Esirkepov, K. Nishihara, S. Bulanov, and F. Pegoraro, *ibid.* **89**, 275002 (2002).
[9] K. Mima, M. S. Jovanovic, Y. Sentoku, Z.-M. Sheng, M. M. Škorić, and T. Sato, Phys. Plasmas **8**, 2349 (2001); Baiwen Li, S. Ishiguro, M. M. Škorić, Min Song, and T. Sato, *ibid.* **12**, 103103 (2005).
[10] J. H. Marburger and R. F. Tooper, Phys. Rev. Lett. **35**, 1001 (1975); C. S. Lai, *ibid.* **36**, 966 (1976); T. Zh. Esirkepov, F. F. Kamenets, S. V. Bulanov, and N. M. Naumova, JETP Lett. **68**, 36 (1998).
[11] V. A. Kozlov, A. G. Litvak, and E. V. Suvorov, Sov. Phys. JETP **49**, 75 (1979); P. K. Kaw, A. Sen, and T. Katsouleas, Phys. Rev. Lett. **68**, 3172 (1992); D. Farina, M. Lontano, and S. Bulanov, Phys. Rev. E **62**, 4146 (2000); D. Farina and S. V. Bulanov, Phys. Rev. Lett. **86**, 5289 (2001); S. Poornakala, A. Das, A. Sen, and P. K. Kaw, Phys. Plasmas **9**, 1820 (2002); S. Poornakala, A. Das, P. K. Kaw, A. Sen, Z. M. Sheng, Y. Sentoku, K. Mima, and K. Nishikawa, *ibid.* **9**, 3802 (2002); M. Lontano, M. Passoni, and S. V. Bulanov, *ibid.* **10**, 639 (2003).
[12] J. I. Gerstein and N. Tzoar, Phys. Rev. Lett. **35**, 934 (1975); N. L. Tsintsadze and D. D. Tskhakaya, Sov. Phys. JETP **45**, 252 (1977); P. K. Shukla, N. N. Rao, M. Y. Yu, and N. L. Tsintsadze, Phys. Rep. **138**, 1 (1986); H. H. Kuehl and C. Y. Zhang, Phys. Rev. E **48**, 1316 (1993); Y. S. Dimant, R. N. Sudan, and

O. B. Shiryaev, Phys. Plasmas **4**, 1489 (1997).
[13] N. M. Naumova, S. V. Bulanov, T. Zh. Esirkepov, D. Farina, K. Nishihara, F. Pegoraro, H. Ruhl, and A. S. Sakharov, Phys. Rev. Lett. **87**, 185004 (2001).
[14] M. Borghesi, S. Bulanov, D. H. Campbell, R. J. Clarke, T. Zh. Esirkepov, M. Galimberti, L. A. Gizzi, A. J. MacKinnon, N. M. Naumova, F. Pegoraro, H. Ruhl, A. Schiavi, and O. Willi, Phys. Rev. Lett. **88**, 135002 (2002).
[15] M. Borghesi, D. H. Campbell, A. Schiavi, M. G. Haines, O. Willi, A. J. MacKinnon, P. Patel, L. A. Gizzi, M. Galimberti, R. J. Clarke, F. Pegoraro, H. Ruhl, and S. Bulanov, Phys. Plasmas **9**, 2214 (2002).
[16] T. Tajima and J. M. Dawson, Phys. Rev. Lett. **43**, 267 (1979).
[17] A. I. Akhiezer and R. V. Polovin, Sov. Phys. JETP **30**, 915 (1956).
[18] T. Zh. Esirkepov, Comput. Phys. Commun. **135**, 144 (2001).
[19] T. Tajima and Y. C. Lee, J. Comput. Phys. **42**, 406 (1981).
[20] E. Esarey, P. Sprangle, M. Pilloff, and J. Krall, J. Opt. Soc. Am. B **12**, 1695 (1995).
[21] S. V. Bulanov, M. Lontano, T. Zh. Esirkepov, F. Pegoraro, and A. M. Pukhov, Phys. Rev. Lett. **76**, 3562 (1996).
[22] S. V. Bulanov, T. Zh. Esirkepov, M. Lontano, and F. Pegoraro, Plasma Phys. Rep. **23**, 660 (1997).
[23] N. M. Naumova, J. Koga, K. Nakajima, T. Tajima, T. Z. Esirkepov, S. V. Bulanov, and F. Pegoraro, Phys. Plasmas **8**, 4149 (2001).
[24] S. V. Bulanov, F. Pegoraro, A. M. Pukhov, and A. S. Sakharov, Phys. Rev. Lett. **78**, 4205 (1997).
[25] G. A. Askar'yan, Sov. Phys. JETP **15**, 8 (1962); Sov. Phys. Usp. **16**, 680 (1973); A. G. Litvak, Sov. Phys. JETP **30**, 344 (1969); C. Max, J. Arons, and A. B. Langdon, Phys. Rev. Lett. **33**, 209 (1974).
[26] N. M. Naumova, S. V. Bulanov, K. Nishihara, T. Zh. Esirkepov, and F. Pegoraro, Phys. Rev. E **65**, 045402(R) (2002).